

Strange regularities in the geometry of myelin nerve-insulation — a possible single cause

Ondwelle short-monograph, No. 1

Robert R. Traill

(late of the *History and Philosophy of Science* Dept., Melbourne University)

email: rrtraill4@dodo-com-au — *Tel.* 61-3-9598-9239

published online by: Ondwelle Publications, 29 Arkaringa Cres., Black Rock 3193, Vic., Australia
March 2005

© Copyright R.R.Traill, 2005.

Users are permitted to use this article for single-copy non-commercial purposes provided that the original authorship is properly and fully attributed to both author and publisher.

If an article is subsequently reproduced or disseminated not in its entirety but only in part or as a derivative work, this must be clearly indicated.

For commercial or multi-copy permissions, please contact Copyright Agency Limited:

Contact details for Copyright Agency Limited (CAL):
email: info@copyright.com.au ; *Tel.:* +61 2 9394 7600; *Fax:* +61 2 9394 7601;
Address: Level 19, 157 Liverpool Street, Sydney, NSW 2000, Australia.

CONTENTS

Strange regularities in the geometry of myelin nerve-insulation — a possible single cause	2
Abstract	2
1. The Peters Quadrant mystery.....	2
2. What could evoke such a virtual-cylinder?	3
3. The Notion of an IR-controlled Virtual Cylinder	4
3.1. An earlier postulate of IR-signals travelling <i>Axially</i>	4
3.2. The Present Basic Model.....	4
3.3. Adequate Reflection?	4
3.4. Historical Precedents from Physics	4
4. Vibration Modes for Axon-cylinders — a notational digression.....	5
4.1. Ideograms, and classification of modes.....	5
4.2. Modes of vibration within films and wire-like cylinders.....	5
5. The Myelination Scenario	6
5.1. The “critical diameter” (d_{crit}) at which myelination starts	6
5.2. Myelin thickness (m) which tends to stay proportional to d	6
5.3. The TE_{11} “(↑↑↑)” mode as a proportion template	7
5.4. Other modes as rival templates.....	7
6. Discussion: — Adding Physics and Knowledge-Theory.....	8
Abbreviations used:	8
References	8

This paper is part of a project to find *sound biological explanations for human mental abilities*. The project soon split into two streams: .

STREAM 1 focussed on realistic *coding-mechanisms for memory* — an area in which lab-work can only scratch the surface, hence rigorous interdisciplinary theory was invoked instead. This led to strong suggestions implicating *molecular coding* — ideas consistent with the theories of *Piaget* and *W.R.Ashby*.

STREAM 2 emerged as the parallel problem of *intercommunication* — but its solutions then unexpectedly also offered explanations to other “unrelated” problems! (Moreover, lab-testing of *these Stream 2 ideas* is much more feasible, so we might now hope for such future investigations).

A summary of the whole project is now available:

<http://www.ondwelle.com/OSM12.pdf> .

3-1-2010

A possible cause for strange regularities in the geometry of myelin (nerve-fibre insulation at cell level)

Robert R. Traill (late of the HPS Dept., Melbourne University)

c/- Ondwelle Publications, 29 Arkaringa Cres., Black Rock 3193, Vic., Australia

Abstract

Myelin layers around axons mysteriously tend to occur in whole-numbers of 360° laps, as first noted by Peters (1964, *J.Cell Biol.*, **20**, 281-296). In principle then, we may imagine an intangible but rigidly-defined coaxial cylindrical border-zone around every myelinating axon — thus creating a predetermined outer radius. Myelination would then be analogous to winding a 16mm-diameter rope into a standard spool for 16mm film — a process stopped by spillage when some *integral* number of “course laps” has been completed. This would accord with the Peters observations.

But what could generate such an elusive unseen border? Unaided chemical effects seem unlikely, but there is an alternative in physics with its “immaterial” fields. Applying optics, it seems there is scope for certain reverberation effects under favourable conditions. This situation could support an intangible pipe-like zone of short-range infra-red standing-wave vibration around the axon, with the distil edge of this zone serving as our limiting border. Such mechanisms might suffice even if they were inefficient or intermittent.

This optics approach also appears to explain: (2) the axon’s minimum “critical diameter” (needed before myelination can begin) and (3) why this differs between central and peripheral nervous systems. (4) “ $g \approx \text{constant}$ ” — why cross-sectional proportions tend to remain constant despite growth; and (5) why some related curve-fitting encounters difficulties — inadvertently confounding several “quantal” lines into one diffuse pattern with poor correlation and misleading parameters.

This “Quadrant” topic is explained again, with illustrations, in the *whole-project-summary* of December 2009:

<http://www.ondwelle.com/OSM12.pdf> .

3 Jan 2010

1. The Peters Quadrant mystery

Any nerve-fibre consists of an **axon** (a long process extending from a neuron cell-body) — and in the case of vertebrates, the larger axons usually become coated by segments of insulating **myelin**.

During axon-growth, the myelin wraps around it as a spiral “bandage”. However there is a *surprising tendency for the start and finish of this spiral to occur close together*, as if the myelin were insisting on running only full-laps of the arena — (Peters, 1964; Webster, 1971, pp353-357).

In seeking a rationale, first imagine a causal field around a myelinating axon such that there is a well-defined border at some definite radial-distance from the axon — a “*virtual*” coaxial cylinder — and suppose that any myelination is forced to stop at that hidden outer radius.

Now re-examine the winding process: Any particular layer is fairly rigidly constant in its thickness. Hence the myelin will fill up any rigidly pre-allocated annular space in a predictable number of wound-on layers. This is analogous to winding rope into a film-spool until the rope *spills* at the angle where the initial “lump” occurs. I.e. start and finish will tend to occur within the same “quadrant”.

For larger fibres, there would be more layers, hence more cumulative-“error” — which would explain the diminished quadrant effect then observed (Fraher, 1972; Waxman and Swadlow, 1976).

2. What could evoke such a virtual-cylinder?

The outer myelin radius “R” could hardly be defined by mechanical means such as microtubules — if only because such devices would disrupt the myelin.

Four other possibilities are depicted in [Table 1](#). Note that the myelin barrier makes chemical effects less likely, and — that gradient criteria would entail awkward threshold-detection with poor precision:

(a) *Chemical gradient?* Unlikely as it suffers from both biases.

(b) *Chemical wave pattern?* [Turing \(1952\)](#) and [Meinhardt \(1982\)](#) together explain zebra stripes and butterfly wing-patterns by invoking wave-interference from the differential diffusion rates of two or more interacting chemicals. However such mechanisms seem unsuited to micron-scale sites, or to myelin barriers.

(c) *Physics-based gradients?* Electrostatic? The attenuation of some incoherent continuous emission? Neither seems likely.

(d) *Physics-based wave-patterns?* Any such waves would probably need to be electromagnetic. And given the scale of the relevant structures (notably $0.5\mu\text{m}$ to $10\mu\text{m}$), we would expect half-wavelengths of comparable size — which implicates infra-red (IR).

Yet IR is very heavily absorbed by aqueous media! Actual figures for pure water show a likely effective reach which varies considerably, but hovers around $20\mu\text{m}$ as a rough average — see [Table 2](#). Now $20\mu\text{m}$ obviously betokens severe absorption as judged by our everyday standards; — but it *would* seem to be tolerable for any neural-construction purposes where the distances surveyed would tend to be less than $10\mu\text{m}$.

(We might also consider the possible relevance of “black body” IR *emissions* ([Traill, 2000, Ch.14](#)). In brief, such emissions are unlikely even to be an issue for wavelengths $<3.2\mu\text{m}$. For wavelengths $>4\mu\text{m}$, the question is debatable since it is less than obvious that physicists’ assumptions about graded micro-oscillators would be valid within bio-media.)

TABLE 1 — assessing four candidate solution-types to explain the postulated *virtual cylinder* seen as bounding myelin-growth

	Chemistry	Physics	border-position?
gradient-threshold	(a) no	(c) no?	vague
wave-pattern	(b) no?	(d) yes	sharp
access through myelin?	poor, vague	very good	

<p style="text-align: center;">Table 2 Local maximum and minimum absorption rates in water, for <i>infra-red</i> light. — after Zolotarev et al. (1969).</p>		
Wavelength in vacuo (μm)	Distance infra-red travels in water before attenuating to $1/e$ (36.8%)	
	<i>local min.</i> (μm)	<i>local max.</i> (μm)
“Near” IR		
1.6		1819
2.93	0.75	
3.8		88.94
4.72	23.77	
5.3		43.04
6.1	3.79	
7.7		18.57
15.0	2.75	
38.0		8.35
“Far” IR		
48.0	7.83	

Table taken from Traill (2000), with the permission of the publisher.

3. The Notion of an IR-controlled Virtual Cylinder

3.1. An earlier postulate of IR-signals travelling *Axially*

As a perhaps-unconnected phenomenon, it was previously suggested that *mature myelin could DOUBLE as a fibre-optic channel* between nodes of Ranvier, and that IR would then probably be involved, (Traill, 1988, 1999).

That IR-transmission model was based on the comparatively safe conceptual ground of the advanced electromagnetic theory of coaxial cables. Thus there were no serious theoretical problems in envisaging IR transmission through the myelin which is a fairly orthodox dielectric. Moreover, reflection at the boundary could either be by “Total Reflection”, or as “metal-like reflection” from the mobile electrons-or-ions of the aqueous solutions adjacent to the myelin.

3.2. The Present Basic Model

In contrast to those axial signals, the IR discussed in this present paper is seen as • travelling *transversely within an ionic aqueous solution* (the axoplasm), • dependent on *sufficient reflection at the axon boundary*, which should • partly maintain the transverse IR as *standing waves*. Meanwhile these standing waves would also • leak extensions of themselves into the surrounding space, forming a concentric coherent *interference-pattern around the axon* — with zero-point nodal surfaces whenever the cosine-like standing-wave happened to be zero.

The non-zero external regions could then be potential growth-areas for myelin (“catalysed” or energised by the coherent IR) — and it would suffice if this happened only intermittently. Meanwhile the zero-surfaces or “moats” would amount to the “virtual cylinders” which *terminate* that growth. (Traill, 1999).

3.3. Adequate Reflection?

Normal mirrors offer >50% reflection. In contrast, this paper centres on supposed reverberation between dielectric interfaces whose mirror-like properties are probably no greater than the reflectivity of a rain-puddle. However a thin film of oil on that same puddle will produce those familiar colour-patches due to interference between reflections from the two weakly-reflecting surfaces; and similar standing-wave patterns could plausibly help control growth — with coherence substituting for strength.

3.4. Historical Precedents from Physics

An alternative view of the same activity is offered by the *in-depth theory of electricity in wire-like conductors*. Here the axial and transverse components are depicted as interacting, if only incidentally. E.g., once myelination has started, we can consider the myelin as a conduit for radiation travelling mainly parallel to the axon (as mentioned above), but also leaking some energy sideways into the axoplasm — basic conditions for passive transverse standing-waves across the axon.

This sideways leakage into the “central core” is simply what routinely happens during electrical activity around-and-within a wire, (Poynting, 1885; Heaviside, 1885, 1887; J.J.Thomson, 1893; Sommerfeld, 1899). Counter-intuitive though it may seem, the main activity is actually *outside* the wire, in the surrounding insulator-dielectric (e.g. in myelin or the pre-myelin “space” — or in air, as radio effects testify). However there is still some activity within the “wire”, especially if it is a *poor* conductor, and that activity will be mostly *transverse!* Transverse, that is, unless the core/wire is a *very-poor* conductor (increasingly dielectric in its properties) and then it can start to carry its own

significant axial-signal component — though without being able to lose the transverse component; (Hondros, 1909; Hondros and Debye, 1910; and Schriever, 1920).

Hence we should not be surprised to find IR standing-waves across the axoplasm, and to find them synchronized with waves outside the axolemma and beyond. It will thus be helpful to summarize some details of such vibrations:

4. Vibration Modes for Axon-cylinders — a notational digression

4.1. Ideograms, and classification of modes

Engineers use names like “ $TM_{p,q}$ ” or “ $TE_{2,2}$ ” to identify various vibrational modes within cylindrical waveguides. Unfortunately the “ p and q ” values change their given-significance according to the shape of the cross-section, so that equivalent patterns are given different names within the different dielectric shapes, thus “ $\circ:TM_{01} \approx \square:TM_{11} \approx \odot:TEM$ ” — to paraphrase Rizzi (1988, p217).

Accordingly I suggest frequent *supplementary* use of simple in-text sketches (of the \mathbf{E} -vectors only), using whatever symbols are offered by available fonts, to distinguish between such modes — with “(…)” depicting an end-on view, “[...]” representing a side-on view with the axis horizontal, or “[...]↓” depicting the side view but with a vertical axis. — Thus “[▷|◁]↓” or “[∩]↓” for the “ $\circ:TM_{01} \approx \square:TM_{11}$ ” just mentioned — with an “(>|<)” end-view.

The classification was first systematically presented by Southworth (1936), and Carson *et al.* (1936). More recent texts include Skilling (1962/1948), Rizzi (1988, Ch.5), and many others. Note that all these accounts are primarily concerned with waves *travelling axially* along the wire, whereas our present concern is mainly with the “cutoff” condition where the *transverse* standing-wave is the only existing component, and travel is zero.

4.2. Modes of vibration within films and wire-like cylinders

Rectangular and 1D cases: In its fundamental vibration, a guitar-string accommodates one *half-wavelength*. Likewise with the light reverberating within the oil-film on water — giving a characteristic colour for each film-thickness. Here the *sine-and-cosine* mathematics is easy even when we take harmonics into account.

Circular cross-sections complicate the mathematics. Bessel functions $J_0(\dots)$, $J_1(\dots)$, and $J_1'(\dots)$ are then appropriate, though qualitatively we can just think of these as distorted *cosine-and-sine* curves.

There are numerous possible modes or “harmonics”, varying in two polar dimensions (\mathbf{r} and φ), and also in the choice of two polarized types “TM” and “TE”). Consider two of these modes:¹

$TE_{1,1}$ (alias $H_{1,1}$) which most resembles the guitar-string and oil-film cases, with its Transverse \mathbf{E} -field looking a bit like this “(↑↑↑)” end-on, and “[↑↑↓↓↑↑↓↓]” side-on. This mode is easiest to establish as it accepts the longest (lowest energy) wavelengths; in fact the cutoff wavelength is given by: $\lambda_c = (1.706) \cdot d \cdot n$ — compared to $\lambda_c = (2.0) \cdot \text{thickness} \cdot n$ for the rectangular equivalent discussed earlier. — (n is the relevant refractive index).

$TM_{0,1}$ (alias $E_{0,1}$). Here the \mathbf{E} -field has an *axial* component (hence the “E”_{0,1} name). It is like a sort of two-ended trumpet — the “[▷|◁]↓” or “[∩]↓” case discussed in section 4.1 above. End-on, it looks like a star-burst, with the E-lines emerging from axial-travel and hitting all parts of the circumference — the “(>|<)”. This mode accepts the second-longest wavelength, with $\lambda_c = (1.306) \cdot d \cdot n$.

¹ Note that travel is always perpendicular to both the \mathbf{E} and \mathbf{H} vibrations. Within such enclosed tubular-guides, any travelling waves are forced to zig-zag, so either \mathbf{E} or \mathbf{H} must have an axial component.

5. The Myelination Scenario

In the above discussion, the quadrant effect was envisaged as occurring when the myelin had *matured*. We may now go back and consider earlier phenomena: — from the start of myelination, to the establishment of the “virtual cylinder” boundary.

Here we may *take it as given* that, before-and-during myelination, the axon diameter (“ d ”) will increase up to some maximum for a given site — presumably due to mechanical and chemical causes such as microfibril packing (Sanchez *et al.*, 1996) — but those mechanisms will not concern us here.

5.1. The “critical diameter” (d_{crit}) at which myelination starts

As often discussed since Duncan (1934), there seems to be a minimum critical diameter of about $1\mu\text{m}$ below which PNS myelination cannot usually occur. For the CNS, the figure is more like $0.2\mu\text{m}$.

If we apply the IR standing-wave hypothesis, then one explanation for d_{crit} is obvious: Myelination cannot start until d becomes big enough to allow a single-loop of *available* electromagnetic vibration to reverberate across the diameter. Evidently then, d_{crit} would depend on the shortest wavelength consistently available at that site, and that wavelength would eventually stimulate a $\text{TE}_{1,1}$ “(↑↑)” vibration — for which $\lambda_{\text{c}} = (1.706) \cdot d \cdot n$.

Assuming that the axoplasm’s refractive index is not greatly different from that of water, we can use the Zolotarev (1969) n -figures for vacuum-wavelengths $\geq 1\mu\text{m}$ — or otherwise assume $n=1.33$. Let us look at two general cases:




(i) *The Optic Nerve and other CNS*. Particularly low values of d_{crit} have been observed in the optic nerve: $0.25\mu\text{m}$ (opossum), $0.245\mu\text{m}$ (mouse), $0.2\mu\text{m}$ (fish), $0.18\mu\text{m}$ (fish) — (Hokoç and Oswald-Cruz, 1978; Bishop *et al.*, 1971; Matheson and Roots, 1988; Tapp, 1974 — respectively). From these we may infer trigger (“cut-off”) wavelengths of $\lambda_{\text{c, (vacuum)}} = 0.567, 0.556, 0.454, \text{ and } 0.408\mu\text{m}$ respectively. Note that these are *not actually IR, but visible light instead*: (green, green, blue, and violet).

Perhaps we should not be surprised to find such wavelengths available within the *optic nerve*! However similar findings can also occur elsewhere in the CNS, such as $d_{\text{crit}} = 0.25\mu\text{m}$ (hedgehog pyramidal), (Bishop *et al.*, 1971), suggesting there is also a *metabolic* source for such wavelengths. Moreover not all CNS findings are so extreme: e.g. $d_{\text{crit}} = 0.5\mu\text{m}$ (hedgehog and cat, optic) (*ibid.*), implying an IR wavelength of $1.13\mu\text{m}$ — and other examples more like PNS figures, which may suggest a PNS-like mechanism in those cases:

(ii) *PNS*. As an example close to the supposed benchmark of $d_{\text{crit}} = 1\mu\text{m}$, much discussed since Duncan (1934), let us take the case of $\text{circumf}_{\text{crit}} = 3\mu\text{m}$ from the scattergram of Arbutnott *et al.* (1980) for the cat hindlimb. Here then, $d_{\text{crit}} = 0.955\mu\text{m}$, implying an IR vacuum-wavelength of $2.10\mu\text{m}$.

If this dichotomy does turn out to be valid and significant, then it suggests that some CNS activity may be based on higher-energy quantum transactions than elsewhere in the nervous system. It might therefore be worth investigating whether such higher energies are intimately connected to the more sophisticated mental activities rather than (e.g.) the more passive routine transmissions.

5.2. Myelin thickness (m) which tends to stay proportional to d

Given the standing-wave hypothesis, we might expect proportions to be maintained. Consider this crude sketch “” of the effects studied so far: The middle “” is a single sine-loop across the axon diameter (d), and the rest represents transverse waves in the surrounding myelin-destined space bounded by “”. (Traill, 1999).

As d grows, any wave which supports this transverse pattern must do so *proportionally* and also match zero-points with d — either by increasing its travelling axial component from zero, or by recruiting other lower-energy waves with their longer wavelengths. Either way, as long as the vibrational mode does not change, we might expect $m \propto d$ for mature myelin — in accordance with the well-known but unexplained observation which dates back to [Donaldson and Hoke \(1905\)](#).

Ideally then, we might hope (i) to calculate exact ratio-values for $m:d:D$ etc., and (ii) to draw a *single straight-line graph* of m against r or d with an extension which passes *through the origin*. However reality is a bit more complicated:

5.3. The TE_{11} “(↑↑↑)” mode as a proportion template

Ignoring some difficulties,² we now assume that the d -and- D boundaries will occur neatly at zero-nodes where $\mathbf{E}_\varphi=0$ (and $\mathbf{H}_r=0$) — and in the TE_{11} mode these are both proportional to $J_1'(k\cdot r)$ — ([Marcuvitz, 1986, p69](#)). Looking at the list of zero-points³ we could thus (*initially ignoring refractive index*) infer that⁴ $M = m/r = (5.331-1.841) / (1.841) = 1.896$.

Next, guessing that $(n_{\text{myelin}} / n_{\text{inner}}) = (1.666/1.333) = 5/4$, we get a prediction of $M \approx 1.517$ — (hence a rather small $g \approx 0.397$). Meanwhile there are further complications:

5.4. Other modes as rival templates

Back in section 5.2, the possibility of mode-change was mentioned. This cannot happen until d has grown enough to allow the shortest available wavelengths to form “overtones”; but eventually the following modes could become available in the sequence shown below — each requiring a re-evaluation of expected- M due to the differing patterns of zero-point ratios³:

- (1) (↑↑↑): $TE_{1,1}$ ($\lambda_c=1.706d$) — nodes at $J_1'(k\cdot r)=0 \rightarrow M \approx 1.52$ ($g \approx 0.397$);
- (2) (>|<): $TM_{0,1}$ ($\lambda_c=1.306d$) — nodes at $J_0(k\cdot r)=0 \rightarrow M \approx 1.04$ ($g \approx 0.491$);
- (3) (<>): $TE_{2,1}$ ($\lambda_c=1.029d$) — nodes at $J_2'(k\cdot r)=0 \rightarrow M \approx 0.96$ ($g \approx 0.511$);
- (4a) (>|<>|<): $TM_{1,1}$ ($\lambda_c=0.82d$) — nodes at $J_1(k\cdot r)=0 \rightarrow M \approx 0.66$ ($g \approx 0.601$);
- (4b) (○): $TE_{0,1}$ ($\lambda_c=0.82d$) — nodes at $J_0'(k\cdot r)=J_1(k\cdot r)=0 \rightarrow M \approx 0.66$ ($g \approx 0.601$);

— (e.g. [Rizzi, 1988](#)). These all assume the use of first and second zero-nodes (for r and R respectively), but further solutions would arise if we also consider other node combinations in each case.

Without taking the actual figures too seriously (in view of the simplifying assumptions²), we can nevertheless see some qualitative features — notably the implied *family* of straight-line m -against- r graphs fanning out from the origin, each with its own gradient. This suggests that existing scattergrams might be confounding these separate lines into one spread-out amorphous shape, so that attempts to fit a single curve to such plots could have been misleading.

² Due to boundary-uncertainties such as *conduction-“skin depth”*, there is some ambiguity about zero point location which I will not attempt to resolve here. Also ideal circularity is rather rare, so that will add some further uncertainty.

³ $J_0(\mathbf{x})=0$ at $x= 2.405, 5.520, 8.654, \dots$ cf. $\cos(\mathbf{x})=0$ at $x=1.571, 4.712, 7.854, \dots$ (i.e. $\pi/2, 3\pi/2, 5\pi/2, \dots$);
 $J_1(\mathbf{x})=0$ at $x= [0], 3.832, 7.106, 10.173, \dots$ cf. $\sin(\mathbf{x})=0$ at $x=[0], 3.1416, 6.2832, 9.4248, \dots$; and
 $J_1'(\mathbf{x})=0$ at $x= 1.841, 5.331, 8.536, 11.706, \dots$; $J_2'(\mathbf{x})=0$ at $x= 3.054, 6.704, 9.969, \dots$. Etc. — (where “'” indicates d/dx — i.e. “gradient of” — for the relevant function).

Just as $\cos'(x) = -\sin(x)$, likewise $J_0'(\mathbf{x}) = -J_1(\mathbf{x})$. However $J_1'(x) \neq -J_2(x)$.

⁴ Here I recommend the use of “ M ” ($=m/r$) rather than the traditional “ g ” ($=d/D$) which arose originally in the very different context of indirect measurement by assay ([Schmitt and Bear, 1937](#)). M now seems better, both cognitively and mathematically. The mutual conversions are obviously $g = 1/(1+M)$ and $M = (g^{-1}-1)$.

6. Discussion: — Adding Physics and Knowledge-Theory

Theory-development here depended partly on theory itself, and partly on data acquired for other purposes; so how valid is that indirect procedure? Such queries are the province of epistemology — a speciality which is often misunderstood (both in its *Perception* and its *Scientific Method* guises), but let us consider the present study from three epistemological viewpoints:

The extreme Popperian view says that it is irrelevant where hypotheses come from, provided they are testable experimentally. The present optics-model does seem to offer ample scope for such testing, though that might be costly. *Practical Popperians* would not waste their resources unless they (or their peers) could at least see some sense in the proposals. Such hypotheses would therefore need some minimum of *prima facie* theoretical validity — and maybe the present optics-hypothesis would meet that criterion also.

A more recent epistemological view (e.g. Thagard, 1992; McCollum, 2000), whilst endorsing experimentation, places comparable weight on internal-consistency of the theoretical notions involved — and typically accepts that, in practice, there may not be a perfect fit in either case. In that context, it seems significant that the present optics-model offers provisional explanations for several phenomena simultaneously, notably: the “quadrant”, “critical diameter”, “ $g \approx \text{constant}$ ” — plus the probable need for IR communication between molecular sites in the brain (Traill, 1999), and the likely ability of myelin to aid such traffic (Traill, 1988, 1999).

It may also be significant that there is a shortage of rival explanations. Thus even if the present account eventually turns out to be wrong, it will at least offer a tangible target meanwhile — as a fairly explicit model of what might control the geometry of myelin, and maybe even control other cell-features and tissues as well.

Abbreviations used:

Algebraic: d = inner diameter, D = outer diameter, r and R = corresponding radii, (\mathbf{r} = radius-variable for $J_n(k \cdot \mathbf{r})$), m = myelin thickness; $g = d/D$; $M = m/r$. p, q = integers. $J_n(\dots)$ = Bessel functions.³

Optics: IR (infra-red). $TE_{2,1}$ (alias $H_{2,1}$), or $TM_{0,1}$ (alias $E_{0,1}$), etc. = vibration modes; see section 4. n = refractive index within relevant medium, and for the relevant frequency. λ = wavelength; λ_c = “cutoff wavelength” (here just short enough to allow reverberation within the given space).

Standard Medical: CNS = Central Nervous System (brain *etc.*); PNS = Peripheral Nervous System.

References

- Arbuthnott, E.R., Boyd, I.A., Kalu, K.U., (1980). “Ultrastructural dimensions of myelinated peripheral nerve fibres in the cat...” *J.Physiol.*, **308**, 125-157.
- Bishop, G.H., Clare, M.H., Landau, W.M., (1971). “The relation of axon sheath thickness to fiber size in the central nervous system of vertebrates”. *Intern. J. Neuroscience*, **2**, 69-78.
- Carson, J.R., Mead, S.P., Schelkunoff, S.A., (1936). Hyper-frequency wave guides — mathematical theory. *Bell System Technical Journal*, **15**(2), 310-333.
- Donaldson, H.H., Hoke, G.W., (1905). “The areas of the axis cylinder and medullary sheath as seen in cross sections of the spinal nerves of vertebrates”. *J.Comp.Neurol.* **15**, 1–.
- Duncan, D., (1934). “A relation between axone diameter and myelination determined by measurement of myelinated spinal root fibers”. *J.Comp. Neur.* **60**, 437-471.
- Fraher, J.P., (1972). “A quantitative study of anterior root fibres during myelination”. *J.Anat.*, **112**, 99-124.

- Heaviside, O., (1885). "On the transmission of energy through wires by the electric current" — in his *Electrical Papers*, **1**, (1892/1970), 434-441.
- Heaviside, O., (1887). "The transfer of energy and its application to wires. Energy-current" — in his *Electrical Papers*, **2**, (1892/1970), 91-97.
- Hokoç, J.N., Oswald-Cruz, E., (1978.). "Quantitative analysis of the opossum's optic nerves". *J.Comp.Neurol.*, **178**, 773-782.
- Hondros, D., (1909). "Über elektromagnetische Drahtwellen". *Annalen der Physik (series 4)*, **30**(15), 905-950.
- Hondros, D., Debye, P., (1910). "Elektromagnetische Wellen an dielektrischen Drähten". *Annalen der Physik (series 4)*, **32**(8), 465-476.
- Marcuvitz, N. (Ed.), (1986). "Transmission-line modes", in *Waveguide Handbook*. New York: McGraw-Hill.
- Matheson, D.F., Roots, B.I., (1988). "Effect of acclimation temperature on the axon and fiber diameter spectra and thickness of myelin of fibers of the optic nerve of goldfish". *Experimental Neurology*, **101**, 29-40.
- McCollum, G., (2000). "Social barriers to a theoretical neuroscience". *Trends in Neuroscience*, **23**, 334-336.
- Meinhardt, H., (1982). *Models of biological pattern formation*. London: Academic Press.
- Peters, A., (1964). "Further observations on the structure of myelin sheaths in the central nervous system". *J.Cell Biol.*, **20**, 281-296.
- Poynting, J.H., (1885). "The connection between electric current and the electric and magnetic inductions in the surrounding field". *Trans. Roy. Soc.*, **176**, 277-306. Also in his *Collected Papers*, (1920), Chelsea: New York, Ch.11, pp.194-223.
- Rizzi, P.A., (1988). *Microwave Engineering*, Prentice-Hall.
- Sánchez, I., Hassinger, L., Paskevich, P.A., Shine, H.D., Nixon, R.A., (1996.). "Oligodendroglia regulate the regional expansion of axon caliber and local accumulation of neurofilaments during development independently of myelin formation". *J.Neuroscience*, **16**, 5095-5105.
- Schmitt, F.O., Bear, R.S., (1937). *J.Cellular and Comp.Physiol.*, **9**, 261-273.
- Schriever, O., (1920). "Elektromagnetische Wellen an dielektrischen Drähten". *Annalen der Physik (series 4)*, **63**(23), 645-673.
- Skilling, H.H., (1962/1948). *Fundamentals of Electric Waves*. London: Wiley.
- Sommerfeld, A., (1899). "Ueber die Fortpflanzung elektromagnetischer Wellen längs eines Drahtes". *Annalen der Physik (series 2)*, **67**(2), 233-290.
- Southworth, G.C., (1936). "Hyper-frequency wave guides..." *Bell System Technical Journal*, **15**(2), 284-309.
- Tapp, R.L., (1974). "Axon numbers and distribution, myelin thickness, and the reconstruction of the compound action potential in the optic nerve of the teleost *Eugerres plumeieri*". *J.Comp.Neurol.*, **153**, 267-274.
- Thagard, P., (1992/1993). *Conceptual Revolutions*. Princeton University Press, NJ.
- Traill, R.R., (1988). "The case that mammalian intelligence is based on sub-molecular coding and fibre-optic capabilities of myelinated nerve axons". *Speculations in Science and Technology*, **11**(3), 173-181.
- Traill, R.R., (1999). *Mind and micro-mechanism*. Melbourne: Ondwelle. [Also pdf: www.ondwelle.com]
- Traill, R.R., (2000). *Physics and philosophy of the mind*. Melbourne: Ondwelle. [Also pdf: www.ondwelle.com]
- Turing, A.M., (1952). "The chemical basis of morphogenesis". *Phil. Trans. Roy. Soc., Lond. B.*, **237**, 37-72.
- Waxman, S.G., Swadlow, H.A., (1976). "Ultrastructure of visual callosal axons in the rabbit". *Experimental Neurology.*, **53**(1), 115-127.
- Webster, H.deF., (1971). "The geometry of peripheral myelin sheaths during their formation and growth in rat sciatic nerves". *J.Cell Biol.*, **48**, 348-367.
- Zolotarev, V.M., Mikhailov, B.A., Alperovich, L.I., Popov, S.I., (1969). "Dispersion and absorption of liquid water in the infrared and radio regions of the spectrum". *Optics and Spectroscopy*. **27**, 430-432.